1-1-2019

Healing of Osteochondral Defects via Endochondral Ossification in an Ovine Model

Helen Lydon
University of Cambridge

Alan Getgood
Fowler Kennedy Sport Medicine Clinic

Frances M.D. Henson
University of Cambridge

CARTILAGE
2019, Vol. 10(1) 94–101

DOI: 10.1177/1947603517713818
journals.sagepub.com/home/CAR
SAGE

Healing of Osteochondral Defects via Endochondral Ossification in an Ovine Model

Helen Lydon[1], Alan Getgood[2], and Frances M. D. Henson[1,3]

Abstract

Objective. The objective of this study was to describe the mechanism of healing of osteochondral defects of the distal femur in the sheep, a commonly used translational model. Information on the healing mechanism be useful to inform the design of tissue engineering devices for joint surface defect repair. *Design*. A retrospective study was conducted examining 7-mm diameter osteochondral defects made in the distal medial femoral condyle of 40 adult female sheep, comprising control animals from 3 separate structures. The healing of the defects was studied at post mortem at up to 26 weeks. *Results*. Osteochondral defects of the distal femur of the sheep heal through endochondral ossification as evidenced by chondrocyte hypertrophy and type X collagen expression. Neocartilage is first formed adjacent to damaged cartilage and then streams over the damaged underlying bone before filling the defect from the base upward. No intramembranous ossification or isolated mesenchymal stem cell aggregates were detected in the healing tissue. No osseous hypertrophy was detected in the defects. *Conclusions*. Osteochondral defects of the medial femoral condyle of the sheep heal via endochondral ossification, with neocartilage first appearing adjacent to damaged cartilage. Unlike the mechanism of healing in fracture repair, neocartilage is eventually formed directly onto damaged bone. There was most variability between animals between 8 and 12 weeks postsurgery. These results should be considered when designing devices to promote defect healing.

Keywords

osteochondral, endochondral ossification, cartilage repair, repair, animal models

Introduction

Synovial joint surface defects are important causes of osteoarthritis (OA), the most prevalent disease of synovial joints, afflicting humans and animals and causing a huge health care, welfare, and economic burden.[1] A considerable amount of research time and effort is directed at devising tissue engineering strategies to enhance joint surface defect healing, including using cell-based therapies, tissue engineering solutions, and small molecule treatment. However, the development of optimal repair strategies is hampered by a lack of full understanding of the underlying mechanisms by which joint surface defects heal. While a number of studies exist in rodents and small animals, relatively little is known of the healing mechanism of osteochondral defects in large animals and, by inference, in man.

Joint surface defects occur either in the cartilage ("chondral" defects) or develop in the cartilage and underlying bone ("osteochondral" defects). Osteochondral defects have healing capacity if they are small and are believed to heal by recruiting nondifferentiated bone marrow–derived stromal/stem cells contained in the bone marrow into the damaged site. In contrast, chondral defects have a poor intrinsic healing capacity. Treatment strategies to heal chondral defects often utilize the bone marrow–derived stromal/stem cell population by accessing the bone marrow through microfracture techniques, which provide cost-effective and functional healing in many cases.[2-4] The precise contribution of the stromal stem cell population to the healing of osteochondral defects, however, is not known, although they may have both a direct and/or indirect (modulatory) effect on the repair tissue.

The mechanism by which osteochondral defects heal has been described in a number of animals, with most work being performed in rabbits. Shapiro *et al*[5]. described the sequence of healing in 3-mm diameter osteochondral defects of the femoral trochlea including an initial fibrin

[1]Department of Surgery, University of Cambridge, Cambridge, UK
[2]Fowler Kennedy Sports Medicine Clinic, London, Ontario, Canada
[3]Department of Veterinary Medicine, University of Cambridge, Cambridge, UK

Corresponding Author:
Frances M. D. Henson, Department of Veterinary Medicine, University of Cambridge, Cambridge, CB3 0ES, UK.
Email: fmdh1@cam.ac.uk

repair, mesenchymal cell recruitment, cartilage formation starting adjacent to the damaged cartilage, and subsequent bone formation. Other work, in larger animals, has described cartilage formation adjacent to the residual damaged cartilage. It has been shown that a number of different parameters can affect both the efficiency of healing and possibly the mechanism of healing, including the position of the defect in the knee joint (with both anatomical considerations[6,7] and biomechanical differences[8] being important), the size and depth of the defect,[9] and the age of the animal.[10]

The sheep is a commonly used translational model for evaluating efficacy of potential treatments for osteochondral defects[7,11,12]; however, the mechanisms by which osteochondral defects heal in sheep are not described. The aim of this study was to describe the temporal sequence of healing of 7-mm diameter osteochondral defects of the distal femur in the sheep in order to provide key information on those processes that are potential targets for therapy.

Materials and Methods

This study received approval from both the Animal Welfare and Ethical Review Board, Cambridge University, and the UK Home Office (Project Licence Number 70/8165).

Animals

Forty skeletally mature female Welsh Mountain Sheep (mean age 3.2 ± 0.8 years) were included in the study, representing the control (untreated empty defect) animals from 3 experiments conducted in our laboratory performed by the same surgical team. The experiments were conducted 12 months apart in 3 cohorts, with the surgical component of the work carried out in the same calendar month each year. The feed, husbandry, and location of the sheep was the same in all animals. The animals were all obtained from the same supplier source.

Animal Anesthesia, Preparation, and Surgical Technique

General anesthesia was induced with an injection of thiopentone (3 mg/kg) and maintenance achieved via inhalational anesthetic of a mixture of isofluorane, nitrous oxide, and oxygen. Perioperative analgesia was provided by preoperative intramuscular carprofen. Antibiotic prophylaxis was given via intramuscular procaine penicillin. The basic surgical procedure was identical for all subjects and performed under strict asepsis. Each stifle was physically examined for any abnormalities while anesthetized. If any gross instability or pathology was found, the animal was excluded from participation within the study.

The animal was placed in a dorsal recumbency position and, following surgical preparation, the left stifle joint opened via a parapatellar approach. Following patella subluxation, a full-thickness 7 mm diameter × 6 mm deep osteochondral defect was created in the medial femoral condyle using a hand drill. The joint was closed in a standard fashion. No splints, casts, or immobilization techniques were used in any animal.

Postoperatively, animals were allowed to fully weight bear, but kept in small pens for 48 hours to reduce ambulation. All animals were housed indoors for the remaining study period in large pens or outdoor in fields, both of which permitted normal ambulation. Animals were killed with an overdose of injectable anesthetic at 1, 2, 4, 8, 12, 18, and 26 weeks postsurgery.

Histology

Specimens were decalcified in formic acid/sodium citrate over 4 weeks. Following complete decalcification, the specimens were dehydrated through a series of ethanol exchanges of increasing concentrations, cleared in xylene, and then embedded in paraffin wax. Sections of 8-µm thickness were made through the central portion of the defect. Sections were stained with toluidine blue and/or Safranin O/Fast Green. A semiquantitative histological analysis was performed as described by Mainil-Varlet *et al*.,[13] based on a semiquantitative scoring system originally described by O'Driscoll *et al*.[14] (**Table 1**). This scoring system has a maximum of 34 points and is suitable for demonstrating longitudinal healing of osteochondral defects in large animal species.[6] Scoring was carried out blindly by one observer (FH).

Immunohistochemistry

Immunohistochemistry was performed as described previously.[11] The following primary antibodies were used in this study: polyclonal rabbit anti type X collagen (ab58632, Abcam, UK, 1 in 200 dilution) and monoclonal mouse anti-PCNA (DAKO, UK). Type X collagen immunostaining was detected with a FITC-conjugated secondary anti-rabbit secondary antibody (Sigma) and PCNA immunostaining was detected with a TRITC-conjugated secondary anti-mouse antibody (Sigma). Normal species-specific serum was used as a control for each antibody.

Results

Weeks 1 to 2: The Osteochondral Defect Is Infilled with Fibrous Tissue

At weeks 1 and 2 after injury, the defect site had filled with blood clot and fibrous tissue. The fibrous tissue was organized

Table 1. Parameters included in semiquantitative histological analysis.

Category	Characteristic	Points
Tissue morphology	Mostly hyaline cartilage	3
	Mostly fibrocartilage	2
	Mostly noncartilage	1
	Noncartilage only	0
Matrix staining	Normal or near normal	3
	Moderate	2
	Slight	1
	None	0
Structural integrity	Normal	4
	Beginning of columnar organization	3
	No organization	2
	Cysts or disruptions	1
	Severe disintegration	0
Chondrocyte clustering	No clusters	2
	<25% of the cells	1
	25% to 100%	0
Formation of tidemark	Complete	4
	76% to 90%	3
	50% to 75%	2
	25% to 49%	1
	<25%	0
Subchondral bone formation	Good	2
	Slight	1
	No formation	0
Architecture of the surface	Normal	3
	Slight fibrillation or irregularity	2
	Moderate fibrillation or irregularity	1
	Severe fibrillation or disruption	0
Filling of the defect	91% to 100%	4
	76% to 90%	3
	51% to 75%	2
	26% to 50%	1
	<25%	0
Lateral integration	Bonded at both ends of graft	2
	Bonded at one end/partially bonded at both sides	1
	Not bonded	0
Basal integration	91% to 100%	3
	70% to 90%	2
	50% to 70%	1
	<50%	0
Inflammation	No inflammation	4
	Slight inflammation	2
	Strong inflammation	0

with a visible surface layer. At the edge of the damaged articular cartilage there was a loss of normal architecture (**Fig. 1A**). The normal chondrocyte arrangement was replaced with a zone of multicellular chondrocyte "clusters" associated with a zone of proteoglycan loss as detected by a reduction in toluidine blue staining at the site.

Weeks 4 to 8: Chondrocytes Form Adjacent to the Edge of Damaged Cartilage and Bone Formation Occurs through Endochondral Ossification

Between weeks 4 and 8, neocartilage was evident at the top edges of the defect immediately adjacent to the edge of the remaining cartilage and the cartilage clusters (**Figs. 1B** and **2**). The cells within the chondrocyte clusters were positively stained for PCNA immunoreactivity indicating active cycling. Close examination of the tissue suggested that these new chondrocytes derived primarily from differentiation of the fibrous tissue clot adjacent to the damaged cartilage. However, there was some suggestion that chondrocytes at the edges of the damaged cartilage were contributing to repair as the orientation of the chondrocytes at the edges of the damaged cartilage was toward the neocartilage rather than the articular surface (**Fig. 2**).

From week 4 onwards, the area in which chondrocytes were seen was now extending toward the base of the defect following the edge of the bone. In defects of increasing age these are covered more of the base of the lesion until they joined with the chondrocytes arising from the opposite side of the lesion by approximately 8 weeks postinjury, effectively lining the exposed bone edges of the defect (**Fig. 3**). Chondrocytes adjacent to the exposed bone edge were observed to be larger and more rounded than the new chondrocytes that were arising toward the top of the defect with a morphology similar to hypertrophic chondrocytes. Positive type X collagen staining in these larger chondrocytes confirmed their identity as hypertrophic chondrocytes (**Fig. 3**). No evidence of intramembranous ossification was detected in any of the sections studied, nor were any cartilage "islands" observed within the fibrous tissue away from the damaged bone edges.

Weeks 8 to 12: Bone Formation Occurs through Endochondral Ossification from the Base and Edges of the Lesion

From week 8 onwards, the healing process continued via a process of endochondral ossification with a gradual increase in the amount of cartilage within the defect (**Fig. 4**). The cartilage formed within the healing tissue did not show any recognizable columnar structure at 8 weeks, but by 12 weeks, the chondrocytes were beginning to become more structured at the edge of the lesion close to the intact cartilage.

Week 18: New Bone Formation Continues and Cartilage Is Removed

At week 18, new bone had been formed at the edges and base of the defect: at this time point a characteristic "v"

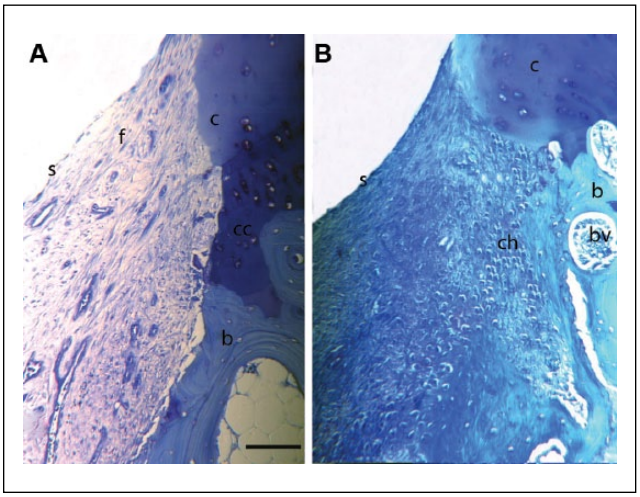

Figure 1. Toluidine blue stained histology sections of the defect edge at (**A**) 1 week and (**B**) 4 weeks postinjury. In both **A** and **B** there is loss of proteoglycan at the cartilage edge and a loss of the normal architecture of the cartilage. Chondrocyte clusters are seen in **B**. In **A**, fibrous tissue fills the defect with a defined surface layer. In **B** the fibrous tissue filling the lesion is being replaced by rounded chondrocytes. c = cartilage edge; f = fibrous tissue in defect; b = bone; s = surface of tissue infill in defect; cc = calcified cartilage; ch = chondrocytes in defect; bv = blood vessel. Bar = 750 μm.

shaped healing lesion was observed (**Fig. 4**). There was evidence of tidemark reformation in the newly formed cartilage only at the edges of the defect and the chondrocytes within this newly formed cartilage had organized into an approximately columnar structure.

Week 26: Healing Is Nearly Complete

Healing was very close to completion at 26 weeks (mean histological score 29.6/34). At 26 weeks the defect had been filled in with cartilage and bone. The cartilage/bone junction was positioned at the correct anatomical site within the cartilage/bone unit; however, the tidemark was not completely reformed in any animal. Within the subchondral bone underneath the newly formed cartilage, there were numerous cartilage remnants remaining that would require further resorption and remodeling in future. No evidence of osseous hypertrophy was found in any sample studied.

Semiquantitative Analysis

A scoring system suitable for scoring the healing of experimental large animal osteochondral defects was used. This scoring system demonstrated that an increase in score correlated with the age of the lesion in these medial femoral condyle lesions (**Fig. 5**). At 1, 2, and 4 weeks of healing the mean healing score (out of a possible total of 34) was 7.6 ± 0.94, 7.3 ± 1.3, and 8.6 ± 1.7, respectively, with the majority of the scoring coming from the integration of the infill material with the intact cartilage edges and the underlying bone. At 8 weeks of healing the mean score had risen to a mean of 14.6 ± 1.7, increasing through a mean of 16.3 ± 2.5 at 12 weeks, a mean of 25 ± 0 at 18 weeks, and ending at 26 weeks with a mean of 29.6 ± 0.63. Between 4 and 8 weeks there was increased scoring for tissue infill and surface integrity and then increasing scoring for morphology, structure, and matrix staining in the later time points. The tidemark was not fully restored at 26 weeks in any animal.

Discussion

Healing of joint surface defects remains a clinical challenge with significant research endeavor directed at optimizing treatment strategies. Understanding the mechanisms behind normal healing is vital to inform therapy selection and experimental design. In this study, we examined the temporal sequence of healing within an osteochondral defect experimentally created in the medial femoral condyle in the sheep and demonstrated that healing of the defect occurs via endochondral ossification. The defect size in this study was 7 mm diameter, which was nearly fully healed within 26 weeks at this anatomical site (cartilage formed in the appropriate place but with some remodeling of subchondral bone and tidemark formation still occurring). These data indicate that a 7-mm osteochondral defect in the medial femoral condyle is able to achieve spontaneous repair and is thus considered as below a "critical size", that is, a defect of a size that cannot spontaneously heal.[15]

Whether or not an experimental defect is small enough to achieve spontaneous repair is extremely important in the evaluation of therapeutic interventions. Various factors play a role in determining whether a defect can spontaneously repair, including the anatomical site of the lesion in the joint (medial femoral condyle lesions are reported to heal more poorly than comparable lesions in the trochlea in the sheep[7] but better in the mini-pig[6]). In the goat, it has been reported that a 6-mm diameter defect in the medial femoral condyle does not undergo spontaneous repair[16]; however, in other studies in sheep an 8.3-mm diameter osteochondral defect in the medial femoral condyle did not heal after 6 months,[9] suggesting that a defect of approximately 8 mm is the size below which spontaneous healing occurs in the medial femoral condyle of adult sheep at 6 months.

These results show that ovine osteochondral healing occurs through a defined sequence of events. Initially the lesion is filled with a hematoma that then rapidly remodels to form a fibrous clot. The first sign of organ-specific tissue is the formation of neocartilage adjacent to the damaged edges of the cartilage. At this stage in the healing process, there was a very similar histological appearance to the healing defects and similar histological scoring in different

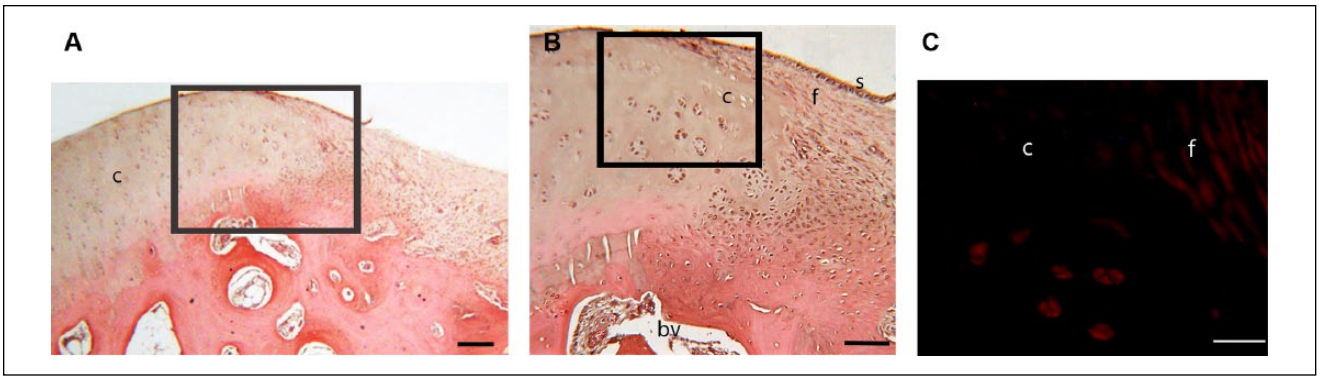

Figure 2. Hematoxylin-eosin stained histology sections of the defect edge at 8 weeks postinjury. (**A**) Low-power view to show structure of the edge of the defect, Bar = 400microns. (**B**) Higher power view of box region of **A** to show presence of multicellular chondrocyte clusters and an apparent recruitment of chondrocytes derived from residual cartilage tissue into the new chondrocytes being produced in the fibrous tissue infill. Bar = 400microns. (**C**) Higher power view of box region of **B** stained with anti-PCNA antibody with a TRITC-labelled secondary antibody. PCNA activity is shown in red. Bar = 250 μm.

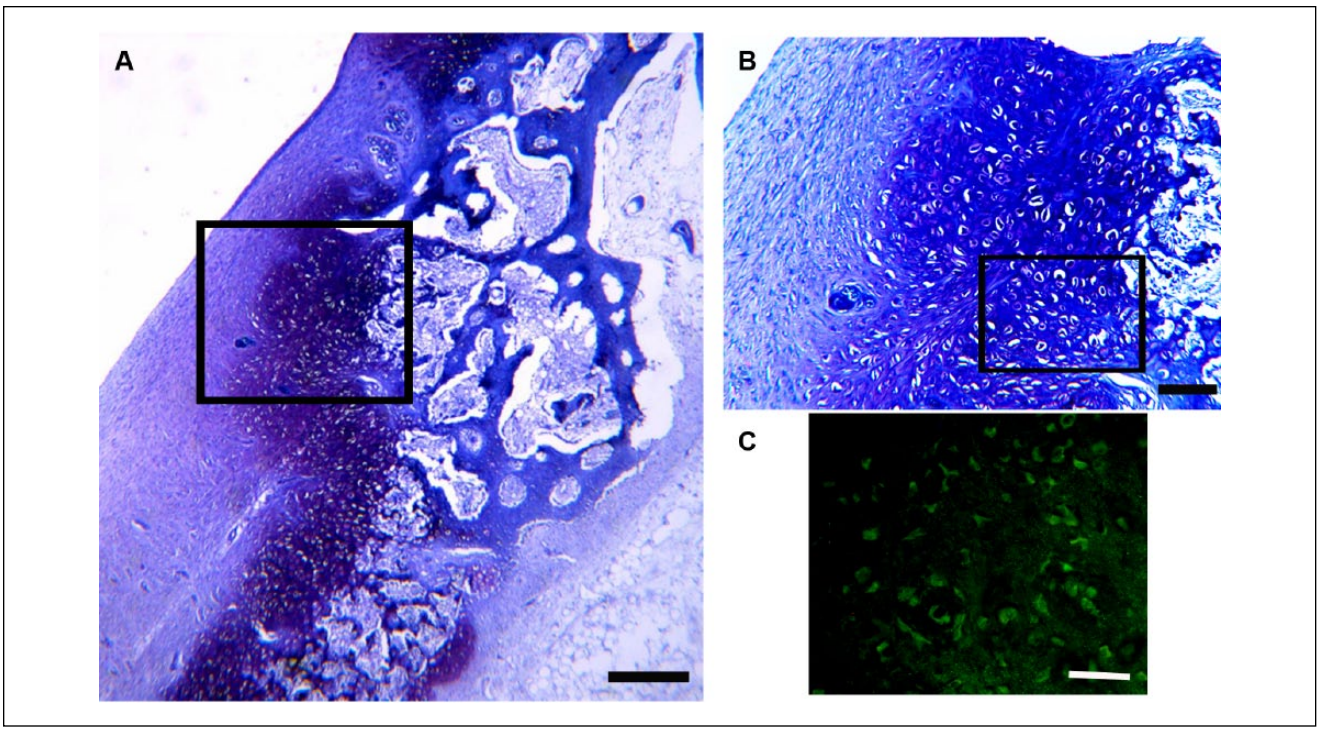

Figure 3. Toluidine blue stained histology section of the defect at 8 weeks postinjury. (**A**) Low-power view to show structure of the edge (red arrows) and base of the defect (black defect). Large rounded cells that are stained more intensely with the toluidine blue can be seen lining the edges and base of the defect (white arrows). Bar = 500 μm. (**B**) Higher power view of box region of **A** to show the appearance of the large rounded cells. Bar = 750 μm. (**C**) Higher power view of box region of **B** stained with anti-type C collagen antibody with a FITC-labelled secondary antibody. Type X collagen is shown in green, confirming the identity of these large rounded cells adjacent to the edge and base of the defect as hypertrophic chondrocytes. Bar = 750 μm. c = cartilage edge; f = fibrous tissue in defect; b = bone; s = surface of tissue infill in defect; hc = hypertrophic chondrocytes; bv = blood vessel.

animals at the same time postsurgery. This neocartilage is then observed, over time, to stream down the edges of the defect supported by the underlying bone, coalescing at the base of the lesion. New bone is produced circumferentially on the edges and base of the lesion via the process of endochondral ossification, as evidenced by the characteristic hypertrophic morphology of the chondrocytes and the expression of type X collagen. In this sheep osteochondral

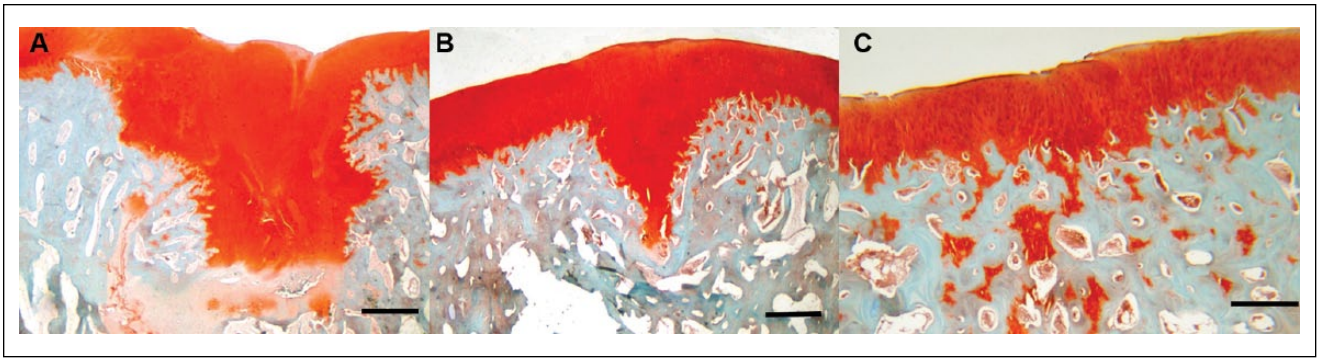

Figure 4. Safranin O stained histology sections of defects at 12 weeks (**A**), 18 weeks (**B**), and 26 weeks (**C**) postinjury. Cartilage is stained in red. At 12 weeks a cartilage plug is filling the defect. At 18 weeks the cartilage plug has reduced in size as the base and sides of the defect become filled in. By 26weeks the cartilage plug has been replaced by bone and the cartilage remaining at the defect site is of a similar depth to the original cartilage. Cartilage remnants are seen within the newly formed bone. Bar = 200 μm.

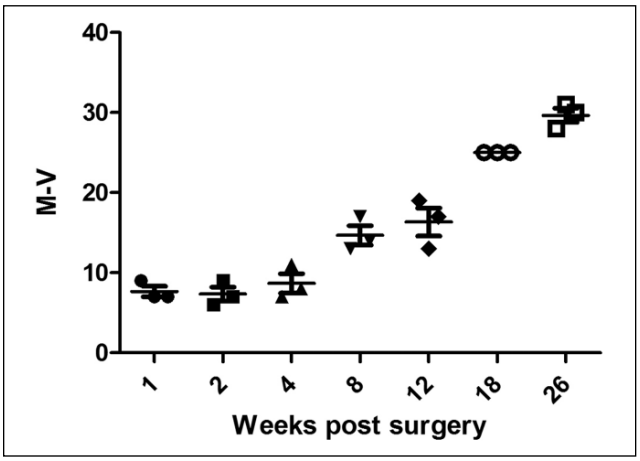

Figure 5. A semi-quantitative analysis was performed on the histological sections from the medial femoral condyle. An increased score correlated with the age of the lesion.

repair process, no evidence of mesenchymal stem cell (MSC) cell condensation was detected in the center of the lesion as had been reported in the rabbit.[5] As healing progressed to weeks 8 and 12, there was a wider difference between individual animals, at 12 weeks the International Cartilage Repair Society scoring varying between 13/34 (38% "healed") and 19/34 (56% "healed"), that is, an 18% variation in healing scores, primarily due to differences in the maturation state of the new cartilage formed. However, by 18 weeks and then at 26 weeks there was a marked reduction in variability, with all animals scoring similarly. These results indicate that, at 26 weeks postsurgery animals have a similar histological appearance in 7 mm defects in the medial femoral condyle. The increased variation between animals at 8 and 12 weeks postsurgery recorded in this study suggests that the interpretation of results of experiments to document osteochondral healing in the medial femoral condyle of sheep with an in-life phase of 8 to 12 weeks is likely to be complicated by individual differences and, as such, are not optimal for such investigations.

The origin of the neocartilage and the cartilage that then covers the exposed bone surface is not known. The neocartilage originates at the junction between the fibrous clot and the damaged cartilage and could arise either from (a) the damaged cartilage edge (via activation of cartilage progenitor cells[17]) or by (b) recruitment and differentiation of MSC (released from the bone marrow). PCNA labelling indicated that the cells within the fibrous clot and the chondrocyte clusters in the damaged cartilage edge are actively cycling. Shapiro *et al*.[5] showed, using longitudinal tritiated thymidine labelling, that there was significant labelling of undifferentiated cells within the fibrous clot, as well as in the damaged cartilage, and concluded that the undifferentiated cells primarily contributed to the regeneration of the defect. However, some histological sections in this study do appear to show a possible contribution of damaged cartilage to new cartilage production and further studies are required to investigate the precise contribution of the chondrocytes and undifferentiated cells in large animal osteochondral healing.

Whatever proves to be the source of the neocartilage, this study demonstrates the importance of the damaged tissue in directing healing. Neocartilage is initially formed adjacent to the damaged cartilage, indicating that, if not directly contributing to the neocartilage production, the damaged cartilage is providing an appropriate structural support for neocartilage production and/or secreting local trophic factors to induce differentiation of undifferentiated cells into cartilage. It is known that adult articular cartilage is a rich source of morphogenic signals upon injury[18,19] and cartilage damage induces activation of factors including bone morphogeneic proteins (BMP) and Wnt signaling proteins within damaged cartilage,[20,21] and released into the local environment, for example, fibroblastic growth factors (FGF).[22]

The importance of the damaged tissue in directing repair is also apparent in the progression of cartilage formation as it lines the edge of the damaged bone prior to infilling the defect. This observation that endochondral ossification occurs upon the damaged bone is unlike the situation during fracture repair, where the cartilage callus is laid down through endochondral ossification on the intact periosteal bone surface rather than on the fractured bone ends,[23] demonstrating that osteochondral repair, in these animals at this anatomical site, occurs in a dissimilar repair environment to that which occurs in fracture repair.

As previously discussed regarding the role of damaged cartilage in neocartilage formation, whether the bone is acting as a physical support and/or as a producer of trophic mediators for chondrogenesis is not known. Differentiation of MSC into chondrocytes is enhanced by increased load[24,25]: we could hypothesize that the junction between fibrous tissue and bone experiences increased load relative to elsewhere in the fibrous tissue within the defect and that the MSC in this area are being influenced by this load differential. The repair tissue/bone interface also represents an area of altered vascularity and oxygen tension within the damaged tissue, and it has been demonstrated, by many authors, that these variables, among many others, can affect cartilage repair processes.[26-28] Clearly, further studies are required to fully characterize the role of bone in osteochondral repair.

There have been few studies that describe longitudinal observations of healing in large animal models, and to the authors' knowledge, there have been no previous studies of longitudinal healing in the medial femoral condyle of the sheep. Jackson *et al.*[15] demonstrated, over 52 weeks in a goat model, that a 6-mm diameter osteochondral defect fails to heal and that progressive, resorption of the defect and subsequent collapse of the defect occur. As observed in this study, clustering of chondrocytes at the edges of the damaged cartilage was noted but endochondral ossification (as determined by toluidine blue staining) was only detected at the base of the lesion. Gotterbarn *et al.*[29] reported that during healing of the medial aspect of the lateral trochlea ridge in mini-pigs endochondral ossification and cartilage streaming was observed at the upper edges of the lesion only.

The results of this study show that endochondral ossification is the mechanism by which osteochondral defects heal in the sheep. The quantitative analysis of the healing shows that there is little variability in the initial stages of healing between animals, but that variability is more marked between 8 and 12 weeks of repair. However, by the end point of this study, 26 weeks, the variability was reduced and the appearance of the healing defects similar. In sheep, unlike in laboratory animals such as mice, there are far more genetic differences between individuals. In this study, we have sought to eliminate individual differences as much as is practically possible, using female sheep of a similar age of the same breed from the same supplier; however, these studies were conducted over a 3-year period (drawn from the control animals of different studies) and the results may be confounded by individual variations.

This finding provides information that may assist the design of tissue engineering strategies to heal osteochondral defects. However, this finding also poses a potential dilemma for strategies that have been used to reduce the deleterious osseous overgrowth that can occur during joint surface defect repair.[30,31] On the basis of the findings reported here, future regenerative therapies should be directed at maintaining chondrocyte phenotype in the chondral layer of the defect once the subchondral bone plate is restored and strategies to inhibit endochondral ossification should be used cautiously.

Acknowledgments and Funding

We would like to acknowledge Dr. Roger Brooks for his technical assistance and the Barcroft Facility, Cambridge.

Declaration of Conflicting Interests

The author(s) declared no potential conflicts of interest with respect to the research, authorship, and/or publication of this article.

Ethical Approval

Ethical approval was not sought for the present study because because it does no included data from human subjects.

Animal Welfare

The present study followed international, national, and/or institutional guidelines for humane animal treatment and complied with relevant legislation.

References

1. Cross M, Smith E, Hoy D, MNolte S, Ackerman I, Frnsen M, *et al*. The global burden of hip and knee osteoarthritis: estimates from the Global Burden of Disease 2010 study. Ann Rheum Dis. 2014;73:1323-30.
2. de Mulder ELW, Gerjon H, van Kuppevelt TH, Daamen WF, Buma P. Similar hyaline-like cartilage repair of osteochondral defects in rabbits using isotropic and anisotropic collagen scaffolds. Tissue Eng Part A. 2014;20:635-45.
3. van Susante JL, Wymenga A, Buma P. Potential healing benefit of an oseoperiosteal bone plug from the proximal tibia on a mosaicplasty donor-site defect in the knee. An experimental study in the goat. Arch Orthop Trauma Surg. 2003;123: 466-70.
4. MIller DJ, Smith MV, Matava MJ, Wright RW, Brophy RH. Microfracture and osteochondral autograft transplantation are cost-effective treatments for articular cartilage lesions of the distal femur. Am J Sports Med. 2015;43:2175-81.
5. Shapiro F, Koide S, Glimcher MJ. Cell origin and differentiation in the repair of full-thickness defects of articular cartilage. J Bone Joint Surg Am. 1993;75:532-53.

6. Jung M, Breusch SJ, Daecke W, Gotterbarm T. The effect of defect localisation on spontaneous repair of osteochondral defects in a Gottingen minipig model: a retrospective analysis of the medial patella groove versus the medial femoral condlye. Lab Anim. 2009;43:191-7.
7. Orth P, Meyer HL, Goebel L, Eldracher M, Ong MF, Cucchiarini M, *et al*. Improved repair of chondral and osteochondral defects in the ovine trochlea compared with the medial condyle. J Orthop Res. 2013;31:1772-9.
8. Duda GN, Maldonado ZM, Klein P, Heller MO, Burns J, Bail H. On the influence of mechanical considerations in osteochondral defect healing. J Biomech. 2005;38:843-51.
9. Nosewicz TL, Reilingh ML, van Dijk N, Duda GN, Schell H. Weightbearing ovine osteochondral defects heal with inadequate subchondral bone plate restoration: implications regarding osteochondral autograft harvesting. Knee Surg Sports Traumalol Arthrosc. 2012;20:1923-30.
10. Bos PK, Verhaar JA, van Osch GJ. Age-related differences in articular cartilage wound healing: a potential role for transforming growth factor beta1 in adult cartilage repair. Adv Exp Med Biol. 2006;585:297-309.
11. Getgood A, Henson F, Skelton C, Herrera E, Brooks R, Fortier LA, *et al*. The augmentation of a collagen/glycosaminoglycan biphasic osteochondral scaffold with platelet-rich plasma and concentrated bone marrow aspirate for osteochondral defect repair in sheep: a pilot study. Cartilage. 2012;3:351-63.
12. Novak T, Fites Gilliland K, Xu X, Worke L, Ciesieski A, Breur G, *et al*. In vivo cellular infiltration and remodelling in a decellularised ovine osteochondral allograft. Tissue Eng Part A. 2016;22:1274-85.
13. Mainil-Varlet P, Aigner T, Brittberg M, Bullough P, Hollander A, Hunziker EB, *et al*. Histological assessment of cartilage repair: a report by the Histology Endpoint Committee of the International Cartilage Repair Society (ICRS). J Bone Joint Surg Am. 2003;85:45-57.
14. O'Driscoll SW, Keeley FW, Salter RB. Durability of regenerated articular cartilage produced by free autogenous periosteal grafts in major full-thickness defects in joint surfaces under the influence of continuous passive motion. A follow-up report at one year. J Bone Joint Surg Am. 1988;70: 595-606.
15. Rudert M. Histological evaluation of osteochondral defects: consideration of animal models with emphasis on the rabbit, experimental setup, follow-up and applied methods. Cells Tissues Organs. 2002;171:229-40.
16. Jackson DW, Lalor PA, Aberman HM, Simon TM. Spontaneous repair of full-thickness defects of articular cartilage in a goat model. A preliminary study. J Bone Joint Surg Am. 2001;83:53.
17. Nelson L, McCarthy HE, Fairclough J, Williams R, Archer CW. Evidence of a viable pool of stem cells within human osteoarthritic cartilage. Cartilage. 2014;5:203-14.
18. Watt FE, Ismail MH, Didangelos A, Peirce M, Vincen TL, Wait R, *et al*. Src and fibroblast growth factor 2 independently regulate signalling and gene expression induced by experimental injury to intact articular cartilage. Arthritis Rheum. 2013;65:397-407.
19. Burleigh A, Chanalaris A, Gardiner MD, Driscoll C, Boruc O, Saklatvala J, *et al*. Joint immobilisation prevents murine osteoarthritis and reveals the highly mechanosensitive nature of protease expression in vivo. Arthritis Rheum. 2012;64:2278-88.
20. Dell'Accio F, De Bari C, El Tail NMF, Barone F, Mitsiadis TA, O'Dowd J, *et al*. Activation of WNT and BMP signalling in adult human articular cartilage following mechanical injury. Arthritis Res Ther. 2006;8:1-13.
21. Dell'Accio F, De Bari C, Eltawil NM, Vanhummelen P, Pitzalis C. Identification of molecular response of articular cartilage to injury by microarray screening: Wnt16 expression and signalling after injury and in osteoarthritis. Arthritis Rheum. 2008;58:1410-21.
22. Chong KW, Chanalaris A, Burgleigh A, Jin H, Watt FE, Saklatvala J, *et al*. Fibroblast growth factor-2 drives changes in gene expression following injury to murine cartilage in vitro and in vivo. Arthritis Rheum. 2013;65:2346-55.
23. Ford JL, Robinson DE, Scammel BE. Endochondral ossification in fracture callus during long bone repair: the localisation of "cavity-lining cells" within the cartilage. J Orthop Res. 2004;22:368-75.
24. Angele P, Yoo JU, Smith C, Mansour J, Jepsen KJ, Nerlich M, *et al*. Cyclic hydrostatic pressure enhances the chondrogenic phenotype of human mesenchymal progenitor cells differentiated in vitro. J Orthop Res. 2003;21:451-7.
25. Terraciano V, Wang N, Moroni L, Park HB, Zhang Z, Mizrahi J, *et al*. Differential response of adult and embryonic mesenchymal progenitor cells to mechanical compression in hydrogels. Stem Cells. 2007;25:2730-8.
26. Babarina AV, Mollers U, Bittner K, Vischer P, Bruckner P. Role of the subchondral vascular system in endochondral ossification: endothelial cell-derived proteinases derepress late cartilage differentiation in vitro. Matrix Biol. 2011;20:205-13.
27. Shang J, Liu H, Li J, Zhou Y. Roles of hypoxia during the chondrogenic differentiation of mesenchymal stem cells. Curr Stem Cell Res Ther. 2014;9:141-7.
28. Gaut C, Sugaya K. Critical review on the physical and mechanical factors involved in tissue engineering of cartilage. Regen Med. 2015;10:665-79.
29. Gotterbarn T, Breusch SJ, Scheider U, Jung M. The minipig model for experimental chondral and osteochondral defect repair in tissue engineering: retrospective analysis of 180 defects. Lab Anim. 2008;42:71-82.
30. Blanke M, Carl HD, Klinger P, Swoboda B, Hennig F, Gelse K. Transplanted chondrocytes inhibit endochondral ossification within cartilage repair tissue. Calcif Tissue Int. 2009;85:421-33.
31. Klinger P, Surmann-Schmitt C, Brem M, Swoboda B, Distler JH, Carl HD, *et al*. Chondromodulin 1 stabilizes the chondrocyte phenotype and inhibits endochondral ossification of porcine cartilage repair tissue. Arthritis Rheum. 2011;63:2712-31.